

# Halogen-Bond-Assisted Guest Inclusion in a Synthetic Cavity\*\*

Hiroki Takezawa, Takashi Murase, Giuseppe Resnati,\* Pierangelo Metrangolo,\* and Makoto Fujita\*

**Abstract:** The confined space inside a self-assembled cage enhanced halogen bonding (XB) between iodoperfluorocarbons (XB donors) and  $\text{NO}_3^-$  anions or  $\text{H}_2\text{O}$  molecules (XB acceptors), as confirmed by NMR spectroscopy in solution and by X-ray crystallography in the solid state. The cavity also bound an XB donor–acceptor pair,  $\text{C}_6\text{F}_5\text{I}_3$  and  $\text{C}_6\text{H}_5\text{NMe}_2$ , in a selective pairwise fashion.

Halogen bonding (XB) is an attractive interaction between electrophilic halogen atoms in organic halides and Lewis bases, such as amines, ketones, ethers, and nucleophilic anions.<sup>[1,2]</sup> This type of interaction has attracted considerable interest, but most studies on XB reported to date have relied solely on solid-state observations<sup>[3]</sup> or theoretical predictions and interpretations.<sup>[4]</sup> Although they also exist in solution, halogen-bonded systems in liquid media have received much less attention.<sup>[5–7]</sup>

Previously, the self-assembled cage **1** (Figure 1) was shown to accommodate molecular aggregates, such as DNA duplexes<sup>[8]</sup> and fluorine aggregates.<sup>[9]</sup> In the confined space of **1**, weak interactions within the aggregates are enhanced, as observed by both NMR spectroscopy and X-ray crystallography. The solution structures (NMR) were consistently the same as the solid-state structures (X-ray). In this study, we investigated halogen-bonded systems in the cavity of cage **1**. We observed clear XB between iodoperfluorocarbons **2** and **3** (XB donors) and  $\text{NO}_3^-$  anions and/or  $\text{H}_2\text{O}$  molecules (XB acceptors). Both NMR spectroscopic and X-ray crystallographic studies suggested that XB assists guest inclusion. We also observed the pair-selective inclusion of an aromatic

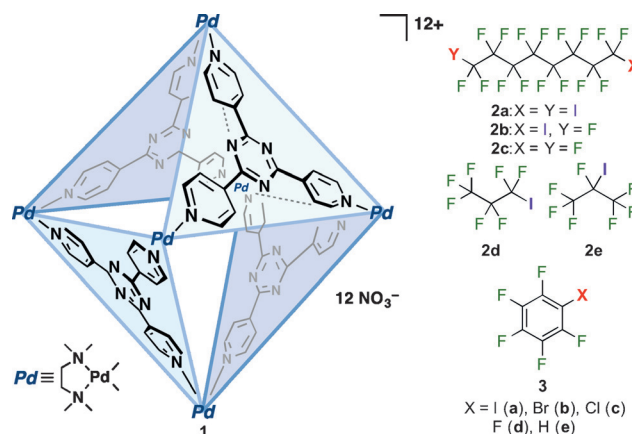


**Figure 1.** Self-assembled coordination cage **1** and perfluorinated alkyl and aryl guests **2** and **3** used in this study.

amine and a polyfluoroaryl iodide. This behavior is indicative of a halogen-bonded guest pair stabilized by the cavity of **1**. The clear observation of XB in solution was supported by X-ray crystallographic analysis in the solid state.

The iodine atom of a perfluoroalkyl iodide ( $\text{R}_\text{F}\text{-I}$ ) is a strong XB-donor site because of the electron-withdrawing nature of the  $\text{R}_\text{F}$  group. We first compared the ability of cage **1** to encapsulate perfluoroalkyl iodides **2a** and **2b** with its ability to encapsulate the perfluorocarbon **2c**, which is devoid of a strong XB-donor site (Figure 1). A suspension of the bisiodide derivative **2a** (5 equiv) in an aqueous solution of cage **1** (5.0 mM) was stirred at 80 °C for 1 h. After the removal of excess solid **2a** by decantation, the  $^1\text{H}$  NMR spectrum showed the formation of a 1:2 host–guest complex **1**(**2a**)<sub>2</sub> in approximately 50 % yield (Figure 2). In the  $^{19}\text{F}$  NMR spectrum, the signals of internal  $\text{CF}_2$  groups (signals *b–d*) were shifted upfield ( $\Delta\delta \approx -2$  ppm), as a consequence of shielding from cage **1**. Unexpectedly, a larger upfield shift ( $\Delta\delta = -6.8$  ppm) was observed for the  $\text{CF}_2$  group adjacent to the iodine atom (signal *a*), despite its less-shielded position. This upfield shift suggests XB with either  $\text{NO}_3^-$  anions or  $\text{H}_2\text{O}$  molecules, which donate electron density to the positively polarized iodine atoms of **2a**.<sup>[6]</sup> Similar upfield shifts were observed for the  $\alpha\text{-CF}_2$  signal of heptafluoro-1-iodopropane (**2d**,  $\Delta\delta = -6.7$  ppm) and the  $\alpha\text{-CF}$  signal of heptafluoro-2-iodopropane (**2e**,  $\Delta\delta = -6.5$  ppm) upon encapsulation in cage **1** to give inclusion complexes **1**(**2d**)<sub>4</sub> and **1**(**2e**)<sub>4</sub>. This result supports the hypothesis that XB involves  $\text{H}_2\text{O}$  molecules or  $\text{NO}_3^-$  anions present in solution and occurs at the portals of cage **1** (see Figure S1 in the Supporting Information).<sup>[6]</sup> The highly positive charge of the cage may also assist in effective XB at the portals.

[\*] Dr. H. Takezawa, Prof. Dr. M. Fujita  
Department of Applied Chemistry  
School of Engineering, The University of Tokyo  
7-3-1 Hongo, Bunkyo-ku, Tokyo 113-8656 (Japan)  
E-mail: mfujita@appchem.t.u-tokyo.ac.jp

Dr. T. Murase  
Department of Material and Biological Chemistry  
Faculty of Science, Yamagata University  
1-4-12 Kojirakawa-machi, Yamagata-shi, Yamagata 990-8560 (Japan)  
Prof. Dr. G. Resnati, Prof. Dr. P. Metrangolo  
Laboratory of Nanostructured Fluorinated Materials (NFMLab)  
Department of Chemistry, Materials, and Chemical Engineering  
“Giulio Natta”, Politecnico di Milano  
Via L. Mancinelli 7, 20131 Milano (Italy)  
E-mail: giuseppe.resnati@polimi.it  
pierangelo.metrangolo@polimi.it

[\*\*] This research was supported by Grants-in-Aid for Specially Promoted Research (24000009) and for Young Scientists (A; 25708008), and by FIRB/MIUR (FLUORIMAGING). H.T. is grateful for a JSPS Research Fellowship for Young Scientists.

Supporting information for this article is available on the WWW under <http://dx.doi.org/10.1002/anie.201500994>.

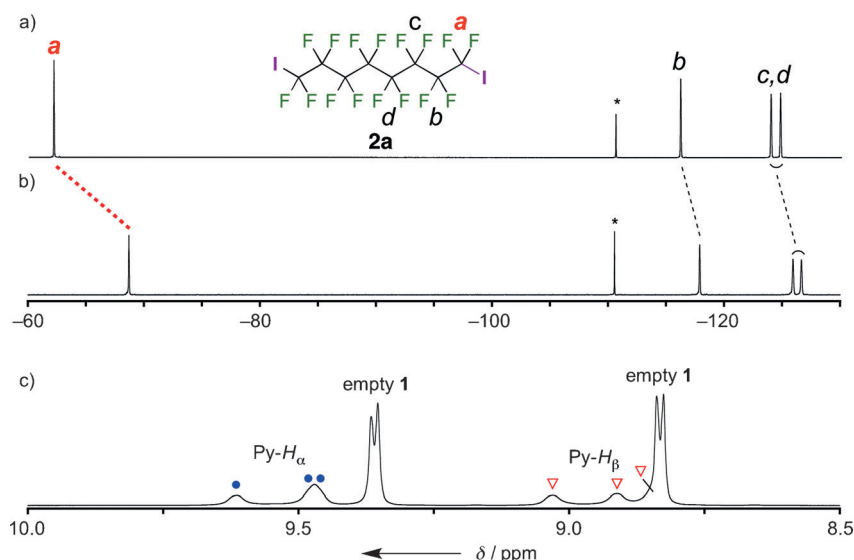


**Figure 2.** a,b)  $^{19}\text{F}$  NMR spectra (470 MHz, 300 K) of **2a** in  $\text{CDCl}_3$  (a) and **1·(2a)<sub>2</sub>** in  $\text{D}_2\text{O}$  (b; \* labels denote signals of the internal standard, 1,3,5-trifluorobenzene, in a capillary tube). c) Expanded  $^1\text{H}$  NMR spectrum (500 MHz, 285 K) of the inclusion complex **1·(2a)<sub>2</sub>** in  $\text{D}_2\text{O}$ .

The Py-*H* signals of cage **1** (Py=4-pyridyl) in the  $^1\text{H}$  NMR spectrum of complex **1·(2a)<sub>2</sub>** were split into three broadened peaks (Figure 2c). This observation is consistent with an orthogonal orientation of the two rodlike molecules of **2a** in the cavity of **1**, which reduces the symmetry of the cage from  $T_d$  to  $D_{2d}$  symmetry.<sup>[10]</sup> The guest geometry is fixed on the NMR timescale presumably because of efficient XB at the portals of cage **1** that pins the iodine atoms in place. In contrast to **2a**, neither 1-iodoperfluorooctane (**2b**) nor perfluorooctane (**2c**) was encapsulated by cage **1**. This result indicates the need for XB to occur at both ends of the guest for inclusion to be possible.

XB of **2a**, **2d**, and **2e** at the portals of cage **1** was directly visualized by X-ray crystallographic analysis (Figure 3; see also Figure S16). From solutions of **1·(2a)<sub>2</sub>**, **1·(2d)<sub>4</sub>**, and **1·(2e)<sub>4</sub>**, single crystals of the complexes were obtained and subjected to a diffraction study. These crystal structures reveal the expected halogen-bonded guest inclusion in cage **1**. In the **1·(2a)<sub>2</sub>** complex, the two guest molecules adopt the predicted orthogonal orientation. All iodine atoms are located at the portals of cage **1** and participate in XB with either  $\text{NO}_3^-$  anions or  $\text{H}_2\text{O}$  molecules. Short  $\text{I}\cdots\text{O}$  contacts are observed in both cases: on average 2.7 Å for  $\text{I}\cdots\text{ONO}_2^-$  and 3.2 Å for  $\text{I}\cdots\text{OH}_2$  (the sum of the van der Waals radii of I and O is 3.5 Å). Furthermore, in **1·(2d)<sub>4</sub>** (see Figure S16) and **1·(2e)<sub>4</sub>** (Figure 3b), all four of the iodine atoms form short contacts with  $\text{NO}_3^-$  anions (on average 3.0 and 2.9 Å for  $\text{I}\cdots\text{ONO}_2^-$  in **1·(2d)<sub>4</sub>** and **1·(2e)<sub>4</sub>**, respectively).<sup>[11]</sup>

XB involving pentafluoriodobenzene,  $\text{C}_6\text{F}_5\text{I}$  (**3a**), was also observed by NMR spectroscopy and X-ray diffraction. The treatment of **3a** with cage **1** in  $\text{D}_2\text{O}$  (room temperature, 30 min) resulted in quantitative formation of the inclusion complex **1·(3a)<sub>4</sub>**, as confirmed by  $^1\text{H}$  and  $^{19}\text{F}$  NMR spectroscopic analysis (see the Supporting Information for details). Again, a significant upfield shift ( $\Delta\delta = -2.6$  ppm) was observed for the fluorine atoms *ortho* to the iodine atom

(see Figure S1). A single crystal suitable for a diffraction study was obtained by slow evaporation of the aqueous solution used for NMR spectroscopy. Crystallographic analysis of **1·(3a)<sub>4</sub>** revealed two disordered structures of the (**3a**)<sub>4</sub> aggregate. In the major structure (ca. 60% occupancy), every molecule of **3a** participates in XB with  $\text{NO}_3^-$  anions, in good agreement with the structures discussed above and with the NMR spectroscopic observations (Figure 4). The  $\text{I}\cdots\text{O}$  distance in this case is 3.1 Å, which is below the sum of the van der Waals radii of the involved atoms (3.5 Å). The X-ray crystal structure also suggests that the electrostatic proximity of  $\text{NO}_3^-$  and  $\text{Pd}^{2+}$  aids effective XB. In the minor structure, **3a** is more deeply accommodated in **1** and XB is not observed (see the Supporting Information).

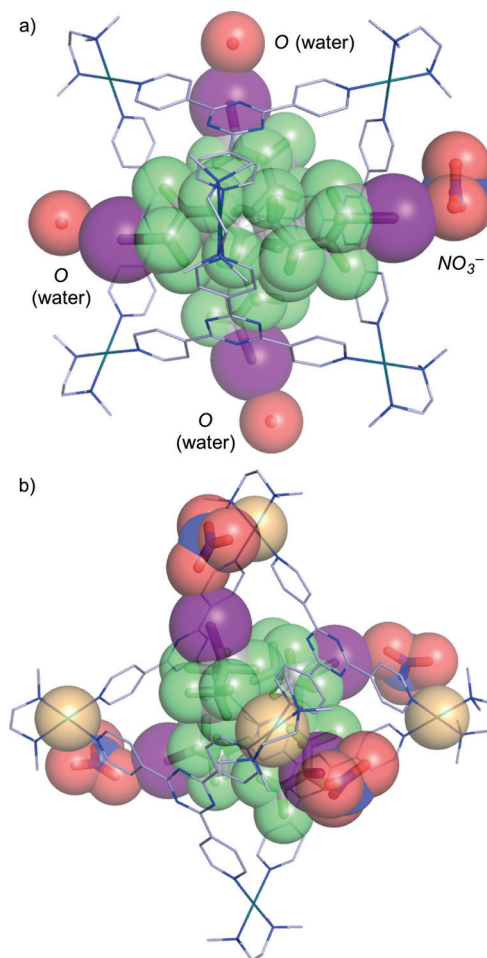


**Figure 3.** X-ray single-crystal structures of a) **1·(2a)<sub>2</sub>** and b) **1·(2e)<sub>4</sub>** (C gray, N blue, O red, F green, I purple, Pd brown). H atoms,  $\text{NO}_3^-$  anions, and water molecules that are not involved in halogen bonding have been omitted for clarity. Only one of the disordered structures is shown for **1·(2e)<sub>4</sub>**.

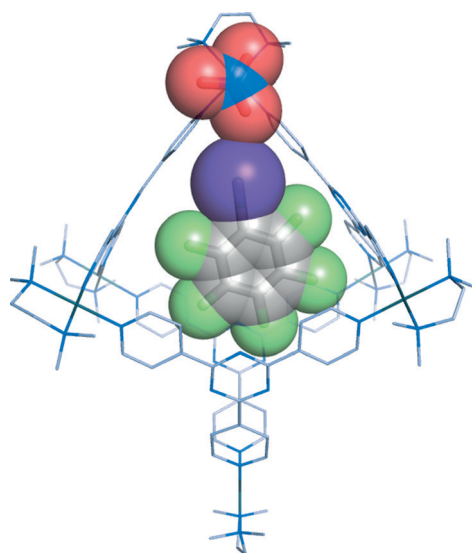
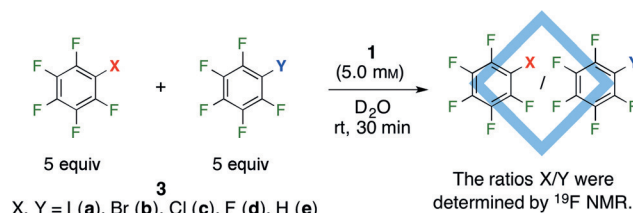


**Figure 4.** X-ray single-crystal structure of **1·(3a)<sub>4</sub>** (C gray, N blue, O red, F green, I purple). Water molecules, NO<sub>3</sub><sup>−</sup> anions that are not involved in halogen bonding, H atoms, and the other three guest molecules, which are identical to that shown owing to symmetry operations, have been omitted for clarity. Only the major disordered structure is shown (see the Supporting Information for details).

From the crystal structure in Figure 4, we assumed that the binding of C<sub>6</sub>F<sub>5</sub>X (**3a–d**: X = I, Br, Cl, and F, respectively) to the cage would become stronger with increasing XB-donor strength (I > Br > Cl > F). To verify this hypothesis, we performed competition experiments with pentafluoroaryl halides **3a–d** (Scheme 1). The treatment of a 1:1 mixture of two different halides (5 equiv each) with a solution of cage **1** (1 equiv) in D<sub>2</sub>O (room temperature, 30 min), followed by measurement of the ratio of included guests by <sup>19</sup>F NMR spectroscopy, clearly showed the relative preferences of the halides to be bound within the cage (Table 1). The measured inclusion efficiency was exactly as expected: **3a** > **3b** > **3c** > **3d**. Furthermore, **3a** and **3b** were more efficiently bound than **3e** (X = H), which can form a medium-strength hydrogen bond.

Finally, we also report a case of the pairwise selective inclusion of an XB donor and an XB acceptor in cage **1** (Figure 5). A suspension of **4** (XB donor, 5.0 equiv) and **5** (XB acceptor, 5.0 equiv) in an aqueous solution of cage **1** (1.0 equiv) was stirred at 80 °C for 1 h. The signal of **4** in the <sup>19</sup>F NMR spectrum of this inclusion complex was significantly shifted upfield (Δδ = −2.7 ppm) and broadened as compared to the corresponding signal in the spectrum of **1·(4)<sub>2</sub>**. Additionally, the signals of **5** in the <sup>1</sup>H NMR spectrum were shifted downfield



**Scheme 1.** Competitive inclusion experiments with pentafluoroaryl halides **3**.

**Table 1:** Relative inclusion selectivities (guest with substituent X/guest with substituent Y) of pentafluoroaryl halides **3** in cage **1**.<sup>[a]</sup>

| X                | Y                |                  |                 |                 |
|------------------|------------------|------------------|-----------------|-----------------|
|                  | Br ( <b>3b</b> ) | Cl ( <b>3c</b> ) | F ( <b>3d</b> ) | H ( <b>3e</b> ) |
| I ( <b>3a</b> )  | 71:29            | 76:24            | 80:20           | 71:29           |
| Br ( <b>3b</b> ) |                  | 63:37            | 76:24           | 62:38           |
| Cl ( <b>3c</b> ) |                  |                  | 66:34           | 50:50           |
| F ( <b>3d</b> )  |                  |                  |                 | 35:65           |

[a] Reaction conditions: cage **1** (5.0 mm in D<sub>2</sub>O, 1 equiv), guests with substituents X and Y (5 equiv each), room temperature, 30 min. Ratios between the two guests were determined from the integral ratio in the <sup>19</sup>F NMR spectrum.

to a much greater extent than those in the spectrum of **1·(5)<sub>4</sub>** (Δδ ≈ 0.78 ppm). Both shifts are indicative of XB. Simple mixing of **4** and **5** in CDCl<sub>3</sub> ([**4**] = 20 mM, [**5**] = 60 mM) caused only subtle signal changes (Δδ = −0.025 ppm for **4** and ca. 0.001 ppm for **5**) in the NMR spectra. Thus, we observed enhancement of XB and pair-selective inclusion within the confined cavity of **1**.

In conclusion, we have clearly observed XB in solution through the inclusion of XB donors in the confined cavity of cage **1**. Our results demonstrate that XB is operative in

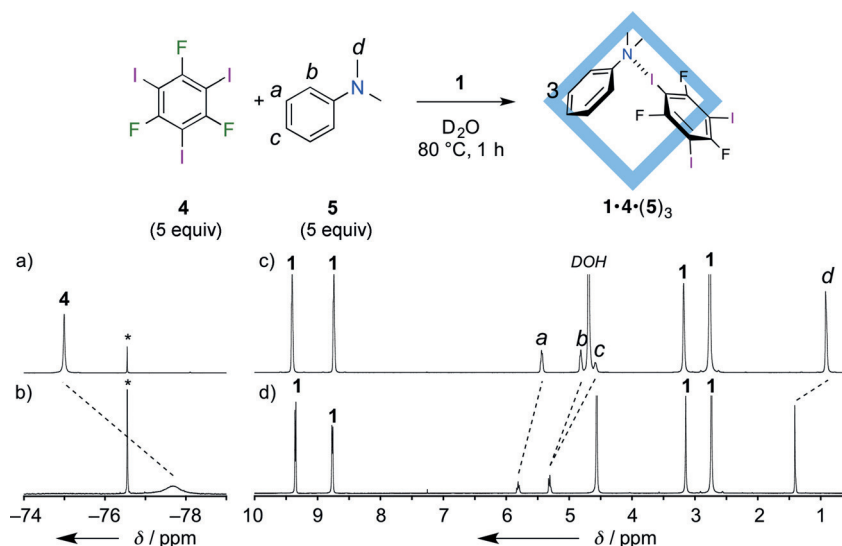


**Figure 5.** Pair-selective formation of a halogen-bonded complex within cage **1**. a, b) <sup>19</sup>F NMR spectra (470 MHz, 305 K, D<sub>2</sub>O) of **1·(4)<sub>2</sub>** (a) and **1·4·(5)<sub>3</sub>** (b); \* labels denote the signals of the internal standard, trifluoroacetic acid, in a capillary tube). c, d) <sup>1</sup>H NMR spectra (500 MHz, 305 K, D<sub>2</sub>O) of **1·(5)<sub>4</sub>** (c) and **1·4·(5)<sub>3</sub>** (d).

solution and may be strong enough to compete with hydrogen bonding in determining the guest to be included in the cavity. The benefits of the confined space of cage **1** are also notable: The cage enhances XB as a result of efficient guest binding (through hydrophobic interactions for organic substrates and electrostatic interactions for anions or solvents), which reduces the entropic disadvantage of donor–acceptor association. Furthermore, the solution geometry of the substrate is reproduced in the solid state as a result of the encapsulation effect, thus making it possible to crystallographically observe halogen-bonded structures similar to those that exist in solution.

**Keywords:** halocarbon compounds · halogen bonding · host–guest interactions · molecular recognition · self-assembly

**How to cite:** *Angew. Chem. Int. Ed.* **2015**, *54*, 8411–8414  
*Angew. Chem.* **2015**, *127*, 8531–8534

- [1] G. R. Desiraju, P. S. Ho, L. Kloo, A. C. Legon, R. Marquardt, P. Metrangolo, P. Politzer, G. Resnati, K. Rissanen, *Pure Appl. Chem.* **2013**, *85*, 1711–1713.
- [2] For selected reviews, see: a) P. Metrangolo, F. Meyer, T. Pilati, G. Resnati, G. Terraneo, *Angew. Chem. Int. Ed.* **2008**, *47*, 6114–6127; *Angew. Chem.* **2008**, *120*, 6206–6220; b) *Halogen Bonding: Fundamentals and Applications* (Eds.: P. Metrangolo, G. Resnati), Springer, Berlin, **2008**; c) G. Cavallo, P. Metrangolo, T. Pilati, G. Resnati, M. Sansotera, G. Terraneo, *Chem. Soc. Rev.* **2010**, *39*, 3772–3783; d) A. Priimagi, G. Cavallo, P. Metrangolo, G. Resnati, *Acc. Chem. Res.* **2013**, *46*, 2686–2695.
- [3] a) J. P. M. Lommerse, A. J. Stone, R. Taylor, F. H. Allen, *J. Am. Chem. Soc.* **1996**, *118*, 3108–3116; b) P. Metrangolo, H. Neukirch, T. Pilati, G. Resnati, *Acc. Chem. Res.* **2005**, *38*, 386–395; c) M. Fourmigué, *Curr. Opin. Sol. State Mater. Sci.* **2009**, *13*, 36–45.
- [4] a) G. Valerio, G. Raos, S. V. Meille, P. Metrangolo, G. Resnati, *J. Phys. Chem. A* **2000**, *104*, 1617–1620; b) W. Wang, N.-B. Wong, W. Zheng, A. Tian, *J. Phys. Chem. A* **2004**, *108*, 1799–1805; c) J.-W. Zou, Y.-J. Jiang, M. Guo, G.-X. Hu, B. Zhang, H.-C. Liu, Q.-S. Yu, *Chem. Eur. J.* **2005**, *11*, 740–751; d) Y.-X. Lu, J.-W. Zou, Y.-H. Wang, Y.-J. Jiang, Q.-S. Yu, *J. Phys. Chem. A* **2007**, *111*, 10781–10788; e) A. R. Voth, P. Khoo, K. Oishi, P. S. Ho, *Nat. Chem.* **2009**, *1*, 74–79.
- [5] For reviews, see: a) M. Erdélyi, *Chem. Soc. Rev.* **2012**, *41*, 3547–3557; b) T. M. Beale, M. G. Ghudzinski, M. G. Sawar, M. S. Taylor, *Chem. Soc. Rev.* **2013**, *42*, 1667–1680.
- [6] a) P. L. Wash, S. Ma, U. Obst, J. Rebek, Jr., *J. Am. Chem. Soc.* **1999**, *121*, 7973–7974; b) P. Metrangolo, W. Panzeri, F. Recupero, G. Resnati, *J. Fluorine Chem.* **2002**, *114*, 27–33; c) M. G. Sarwar, B. Dragisic, L. J. Salsberg, C. Gouliaras, M. S. Taylor, *J. Am. Chem. Soc.* **2010**, *132*, 1646–1653; d) D. A. Smith, L. Brammer, C. A. Hunter, R. N. Perutz, *J. Am. Chem. Soc.* **2014**, *136*, 1288–1291.
- [7] a) H. S. El-Sheshtawy, B. S. Bassil, K. I. Assaf, U. Kortz, W. M. Nau, *J. Am. Chem. Soc.* **2012**, *134*, 19935–19941; b) M. G. Sarwar, D. Ajami, G. Theodorakopoulos, I. D. Petsalakis, J. Rebek, Jr., *J. Am. Chem. Soc.* **2013**, *135*, 13672–13675; c) S. Castro-Fernández, I. R. Lahoz, A. L. Llamas-Saiz, J. L. Alonso-Gómez, M.-M. Cid, A. Navarro-Vázquez, *Org. Lett.* **2014**, *16*, 1136–1139; d) M. J. Langton, S. W. Robinson, I. Marques, V. Félix, P. D. Beer, *Nat. Chem.* **2014**, *6*, 1039–1043.
- [8] a) T. Sawada, M. Yoshizawa, S. Sato, M. Fujita, *Nat. Chem.* **2009**, *1*, 53–56; b) T. Sawada, M. Fujita, *J. Am. Chem. Soc.* **2010**, *132*, 7194–7201.
- [9] H. Takezawa, T. Murase, G. Resnati, P. Metrangolo, M. Fujita, *J. Am. Chem. Soc.* **2014**, *136*, 1786–1788.
- [10] T. Kusakawa, M. Yoshizawa, M. Fujita, *Angew. Chem. Int. Ed.* **2001**, *40*, 1879–1884; *Angew. Chem.* **2001**, *113*, 1931–1936.
- [11] Halogen-bond formation in **1**·(**2a**)<sub>2</sub>, **1**·(**2d**)<sub>4</sub>, and **1**·(**2e**)<sub>4</sub> was also supported by IR spectroscopy (see the Supporting Information).
- [12] G. M. Sheldrick, *Acta Crystallogr. Sect. A* **2008**, *64*, 112–122.

Received: February 2, 2015

Published online: May 27, 2015